Photo- *vs.* mechano-induced polymorphism in the bromide salt of 4-amino-cinnamic acid, and single crystal to single crystal [2+2] photoreactivity.

Simone d'Agostino,[†,*] Paola Taddei,[‡,*] Elisa Boanini,[†] Dario Braga[†] and Fabrizia Grepioni[†]

[†] Dipartimento di Chimica G. Ciamician, Università di Bologna, Via F. Selmi 2, 40126 Bologna, Italy.

[‡] Dipartimento di Scienze Biomediche e Neuromotorie, Università di Bologna, Via Belmeloro 8/2, 40126 Bologna, Italy.

Table of contents

Synthesis..... S2
Crystal structure determination and refinement details..... S2
Crystal packing features for [**1**H]Br form A, C B, and α-[$\mathbf{1}_2H_2$]Br_2..... S3
Overlay of [**1**H]Br form A and C..... S5
Geometrical parameters used for the evaluation of photoreactivity..... S5
Solid State Photoreactions..... S5
Rietveld details..... S6
Hot Stage and Cross-polarized optical Microscopy..... S7
Scanning Electron Microscopy..... S7
Hirshfeld Surface analysis and 2D FingerPrint Plots..... S8
Hydrogen bond variations over the course of photoreaction [**1**H]Br form B → α-[$\mathbf{1}_2H_2$]Br_2..... S9
Cell constant variations over the course of photoreaction [**1**H]Br form B → α-[$\mathbf{1}_2H_2$]Br_2..... S9
Dimer content variations over the course of photoreaction [**1**H]Br form B → α-[$\mathbf{1}_2H_2$]Br_2..... S10
Powder X-ray diffraction S10
FTIR spectroscopy..... S11
Raman spectroscopy..... S11
NMR spectroscopy..... S13
References..... S14

Synthesis. All reactants and reagents were purchased from Sigma-Aldrich and used without further purification. Bi-distilled water was used.

[**1**H]Br form A: 200 mg (1.23 mmol) of 4-aminocinnamic acid (**1**) were added to aqueous HBr (pH *ca.* 2-3); the resulting suspension was sonicated until a clear solution was obtained, which was left to slowly evaporate in the dark. Pale yellow crystals suitable for X-ray crystal diffraction were obtained over a period of 1 week.

[**1**H]Br form B: same procedure as before, but the clear solution was boiled for 10 minutes. Alternatively [**1**H]Br form B can be obtained *via* mechanochemical conversion by manually grinding for few minutes single crystals of [**1**H]Br form A.

α-[$\mathbf{1}_2H_2$]Br_2: Single crystals or polycrystalline powders of [**1**H]Br form B were irradiated overnight with a UV LED (see below). Single crystals suitable for X-ray diffraction were obtained through the SCSC transformation or *via* recrystallization from water in the presence of a few drops of HBr.

Crystal structure determination. Single-crystal data for all salts were collected at RT on an Oxford X'Calibur S CCD diffractometer equipped with a graphite monochromator (Mo-K_α radiation, λ = 0.71073Å). Data collection and refinement details are listed in Table SI-1. All non-hydrogen atoms were refined anisotropically. H_{CH} atoms for all compounds were added in calculated positions and refined riding on their respective carbon atoms; H_{OH} and H_{NH} atoms were either directly located or, when not possible, added in calculated positions. SHELX97[1] was used for structure solution and refinement on F^2. The program Mercury[2] was used to calculate intermolecular interactions and for molecular graphics. Crystal data can be obtained free of charge via www.ccdc.cam.ac.uk/conts/retrieving.htmL (or from the Cambridge Crystallographic Data Centre, 12 Union Road, Cambridge CB21EZ, UK; fax: (+44)1223-336-033; or e-mail: deposit@ccdc.cam.ac.uk). CCDC numbers 1532845-1532851. Crystal structures of partially reacted crystals were treated as follows: (i) upon irradiation, new electron density peaks, consistent with formation of the photoproduct, appeared in the Delta Fourier Map. (ii) The C-atoms of reactant and product were treated as disordered over two positions: first an occupancy factor was refined, keeping the thermal parameters fixed, then the occupancy factor was kept at a fixed value, and the C atoms refined isotropically. (iii) The carboxylic acid and part of the aminophenyl groups were modeled accordingly: an average position of the two conformations was assumed, and the atoms were refined anisotropically.

Table SI-1. Crystal data and details of measurements for crystalline [**1**H]Br form A, [**1**H]Br form C, [**1**H]Br form B and for each stage of its photodimerization up to the complete conversion to α-[$\mathbf{1}_2H_2$]Br_2.

	[1H]Br form A	**[1H]Br form C**	**[1H]Br form B**	**$B_{0.88}\cdot\alpha_{0.12}$**	**$B_{0.58}\cdot\alpha_{0.42}$**	**$B_{0.14}\cdot\alpha_{0.86}$**	**α-[1_2H_2]Br_2**
Formula	$C_9H_{10}BrNO_2$	$C_9H_{10}BrNO_2$	$C_9H_{10}BrNO_2$	$C_9H_{10}BrNO_2$	$C_9H_{10}BrNO_2$	$C_9H_{10}BrNO_2$	$C_9H_{10}BrNO_2$
fw	244.09	244.09	244.09	244.09	244.09	244.09	244.09
Cryst. System	monoclinic	monoclinic	monoclinic	monoclinic	monoclinic	monoclinic	monoclinic
Space group	P21/c	P21/c	P21/c	P21/c	P21/c	P21/c	P21/c
Z	4	4	4	4	4	4	4
a (Å)	4.4248(5)	4.2055(4)	5.8723(3)	5.905(5)	5.9276(5)	6.0173(3)	5.9966(3)
b (Å)	27.804(4)	29.199(3)	8.8268(6)	8.829(5)	8.7714(9)	8.7413(5)	8.7103(5)
c (Å)	8.1876(8)	8.1932(7)	18.8691(15)	18.631(5)	18.352(3)	17.8627(16)	17.850(2)
α (deg)	90	90	90	90	90	90	90
β (deg)	104.433(11)	92.342(7)	92.660(5)	92.573(5)	92.360(13)	92.196(5)	92.284(6)
γ (deg)	90	90	90	90	90	90	90
V ($Å^3$)	975.5(2)	1005.27(17)	977.00(11)	970.4(10)	953.4(2)	938.87(11)	931.59(13)
D_{calc} (g/cm^3)	1.662	1.613	1.659	1.671	1.701	1.727	1.740
μ (mm^{-1})	4.180	4.056	4.174	4.202	4.277	4.343	4.377
Measd reflns	4284	7347	4165	3888	4007	4123	4102
Indep reflns	2236	2407	2215	2198	2185	2143	2168
R_1[on F_0^2, I>2σ(I)]	0.0450	0.1110	0.0484	0.0506	0.0550	0.0507	0.0575
wR_2 (all data)	0.1162	0.2735	0.1116	0.1073	0.1146	0.1056	0.1489

Crystal packing features for [1H]Br form A, C, B, and α-[1_2H_2]Br_2.

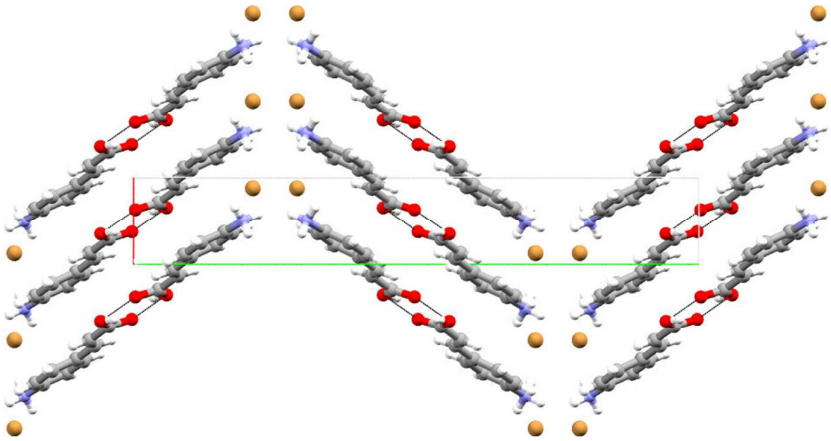

Figure SI-1. Packing diagram of [**1**H]Br form A viewed along the c-axis. The crystal structure is characterized by the presence of carboxylic acid homosynthons $R_2^2(6)$ [$O_{C=O}\cdots O_{OH}$ = 2.637(18) Å]; and interactions between the cationic unit $[\mathbf{1}H]^+$ and Br^- [$NH_3^+\cdots Br^-$ = 3.240(3) Å].

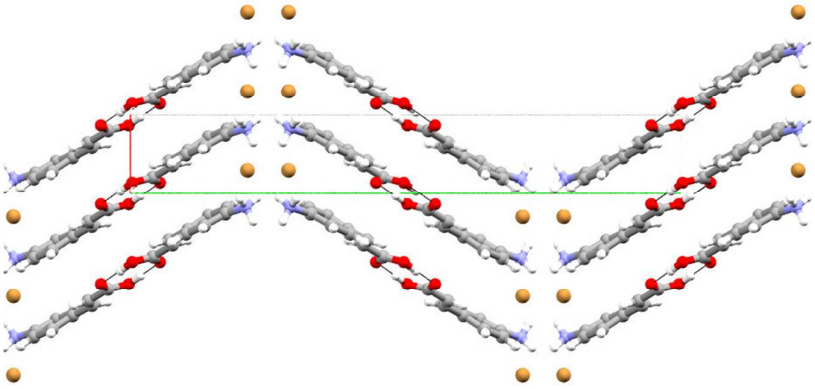

Figure SI-2. Packing diagram of [**1**H]Br form C viewed along the c-axis, showing the carboxylic acid homosynthons $R_2^2(6)$ [$O_{C=O}\cdots O_{OH}$ = 2.634(5) Å] and interactions between the cationic unit $[\mathbf{1}H]^+$ and Br^- [$NH_3^+\cdots Br^-$ = 3.300(11)-3.348(10) Å].

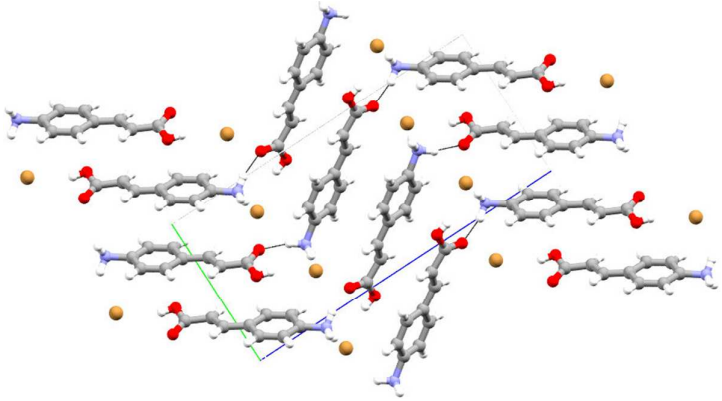

Figure SI-3. Packing diagram of [**1**H]Br form B viewed along the a-axis. The crystal structure features charge assisted hydrogen bonds [$NH_3^+\cdots O_{C=O}$= 2.770(5) Å, and $O_{OH}\cdots Br^-$ = 3.248(4) Å] and interactions between the cationic unit $[\mathbf{1}H]^+$ and Br^- [$NH_3^+\cdots Br^-$ = 3.248(4) Å].

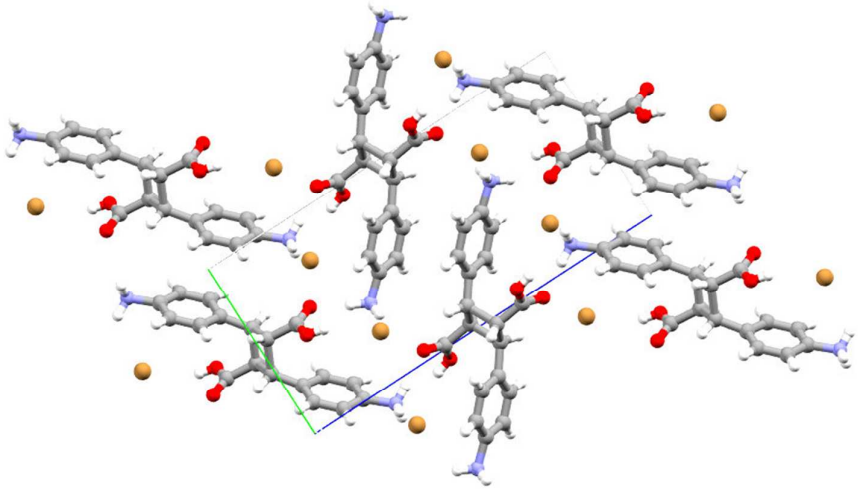

Figure SI-4. Packing diagram of α-[$\mathbf{1}_2H_2$]Br_2 viewed along the a-axis showing charge assisted hydrogen bonds [$NH_3^+\cdots O_{C=O}$= 2.852(3) Å, and $O_{OH}\cdots Br^-$ = 3.286(2) Å] and interactions between the cationic unit $[\mathbf{1}H]^+$ and Br^- [$NH_3^+\cdots Br^-$ = 3.279(1) Å].

Overlay of [1H]Br form A and C

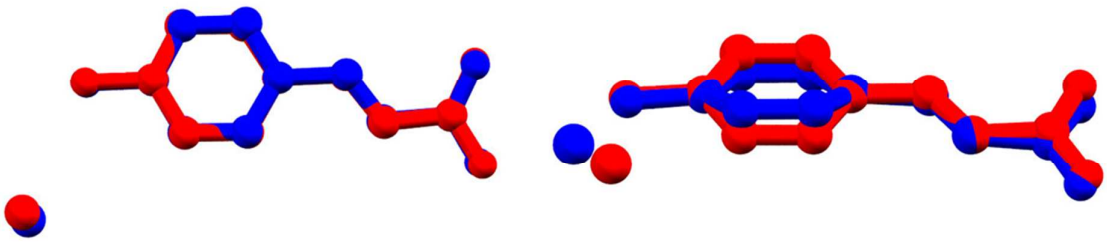

Figure SI-5. Overlay of the molecular structures of crystalline [**1**H]Br Form A (red) and B (blue). Top (left) and side (right) views show the subtle differences in the conformations. H-atoms omitted for clarity.

Scheme 1. Geometrical parameters[3,4] used to evaluate the photoreactivity of all the crystalline compounds described in this study.

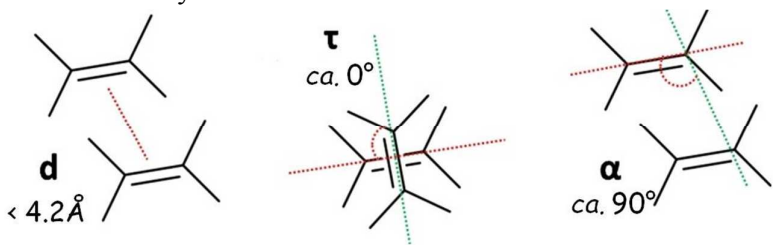

Table SI-2. Types of arrangements observed in crystalline [**1**H]Br form A, C and B, together with their relevant geometrical parameters used for the evaluation of photoreactivity.

	type	**d (Å)**	**α (°)**	**τ (°)**
[**1**H]Br form A	β	4.425(6)	64.5(3)	0
[**1**H]Br form C	β	4.210(1)	78.65(6)	0
[**1**H]Br form B	α	3.618(6)	91.1(3)	0

Arrangements for two cationic units $\mathbf{1}H^+$: α = head-to-tail; β = head-to-head.

Solid State Photoreactions. Single crystals samples were irradiated using a UV-LED (*Led EnginLZ1-10UV00-0000)* with λ = 365 nm and placed at a distance of 1 cm. Powder samples of [**1**H]Br form B were placed onto a flat sample holder and irradiated using two *Led EnginLZ1-10UV00-0000* (λ = 365 nm) placed at a distance of 2 cm. KBr pellets used for FTIR (see below) were irradiated directly in the sample holder using 2 UV-LED (LED ENGINE LZ1-10UV00-0000, λ = 365 nm) placed at a distance of 1 cm each.

Rietveld details. For refinement purposes X-ray powder diffractograms in the 2θ range 5–60° (step size, 0.003°; time/step, 99s; 0.02 rad soller; V x A 40 × 40) were collected on a Panalytical X'Pert PRO automated diffractometer operated in transmission mode (capillary spinner) and equipped with a Pixel detector. Powder diffraction data were analyzed with the software TOPAS4.1.[5] A shifted Chebyshev function with 7 parameters and a Pseudo–Voigt function (TCHZ type) were used to fit background and peak shape, respectively. A spherical harmonics model was used to describe the preferred orientation. An overall thermal parameter for the C, N, O atoms was adopted. Refinements converged with GOF = 4.3, R_{wp} = 9.4%, R_{exp} = 2.2%; GOF = 2.5, R_{wp} = 5.3%, R_{exp} = 2.1 %; GOF = 2.3, R_{wp} = 5.4 %, R_{exp} = 2.2 %. Figure SI-6 shows experimental, calculated and difference curves.

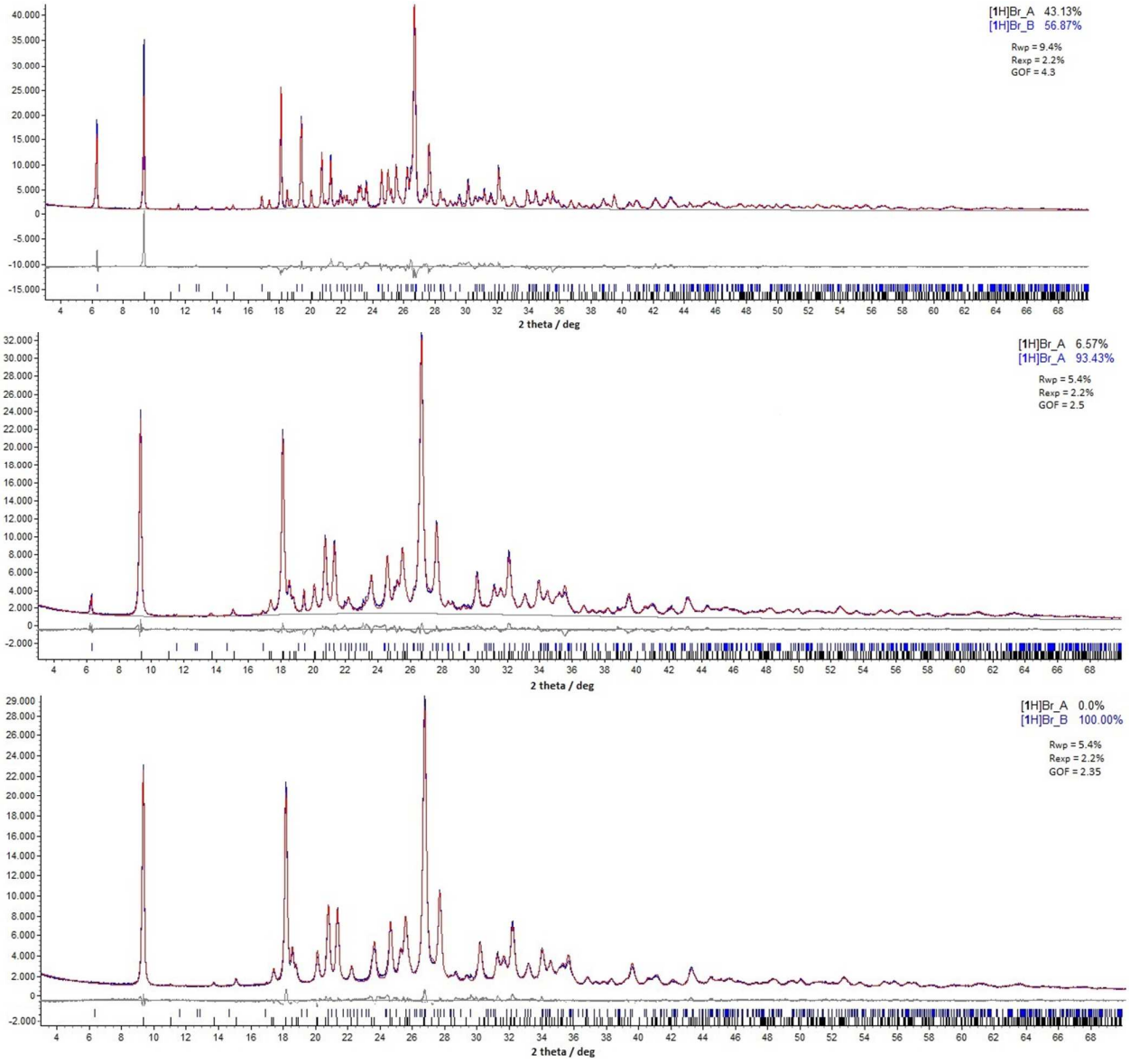

Figure SI-6. Experimental (blue), calculated (red) and difference (grey) patterns for each step of conversion from [**1**H]Br form A to [**1**H]Br form B.

Hot Stage and Cross-polarized Optical Microscopy. Hot Stage experiments were carried out using a Linkam TMS94 device connected to a Linkam LTS350 platinum plate and equipped with polarizing filters. Images were collected with the imaging software Cell, from an Olympus BX41 stereomicroscope.

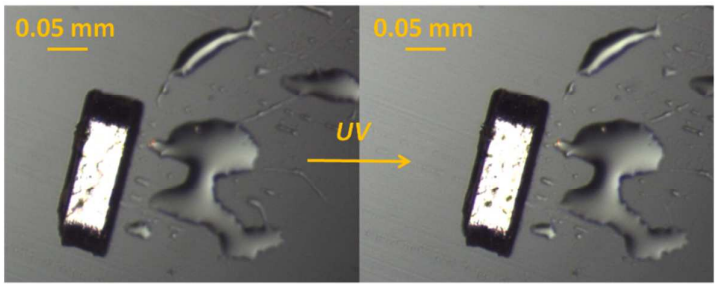

Figure SI-7. Cross-Polarized optical microscope pictures showing single crystals of [**1**H]Br form B before and after overnight UV irradiation corresponding to α-[$\mathbf{1}_2H_2$]Br_2.

Scanning Electron Microscopy. Morphological investigations of crystals were performed using a HITACHI S-2400 scanning electron microscope operating at 15 kV. The samples were observed as-prepared and not sputter coated before examination. Sample preparation is as follows: single crystals were selected directly from the mother liquor and sticked on conductive adhesive tape (carbon) on stub. For this reason it is possible to see on the crystal surface the presence of smaller crystals or traces of polycrystalline samples. UV irradiation was performed *in situ*.

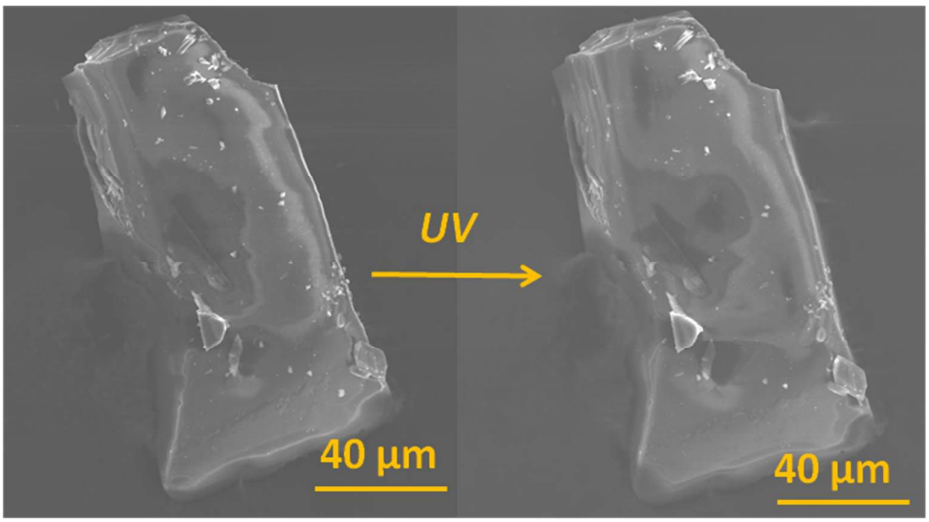

Figure SI-8. SEM micrographs taken on a single crystal of [**1**H]Br form B before and after UV irradiation corresponding to α-[$\mathbf{1}_2H_2$]Br_2.

Hirshfeld Surfaces and 2d FingerPrint Plots. The intermolecular interactions were analyzed in the crystal structure of [**1**H]Br form B and for its related photoproduct α-[1_2H_2]Br_2 to futher explore similarities and differences of those structures. Hirshfeld surfaces were calculated with the software Crystal Explorer[6] for the α-arrangement detected in [**1**H]Br form B and for the corresponding photoproduct α-[$\mathbf{1}_2H_2$]Br_2 (Figure SI-5). As shown by the extracted 2d fingerprinplot[7] (graphical representations of the short contacts distributions in the reactant and product lattices) the overall interaction patterns are very similar (Figure SI-9) since the packings are isostructural.

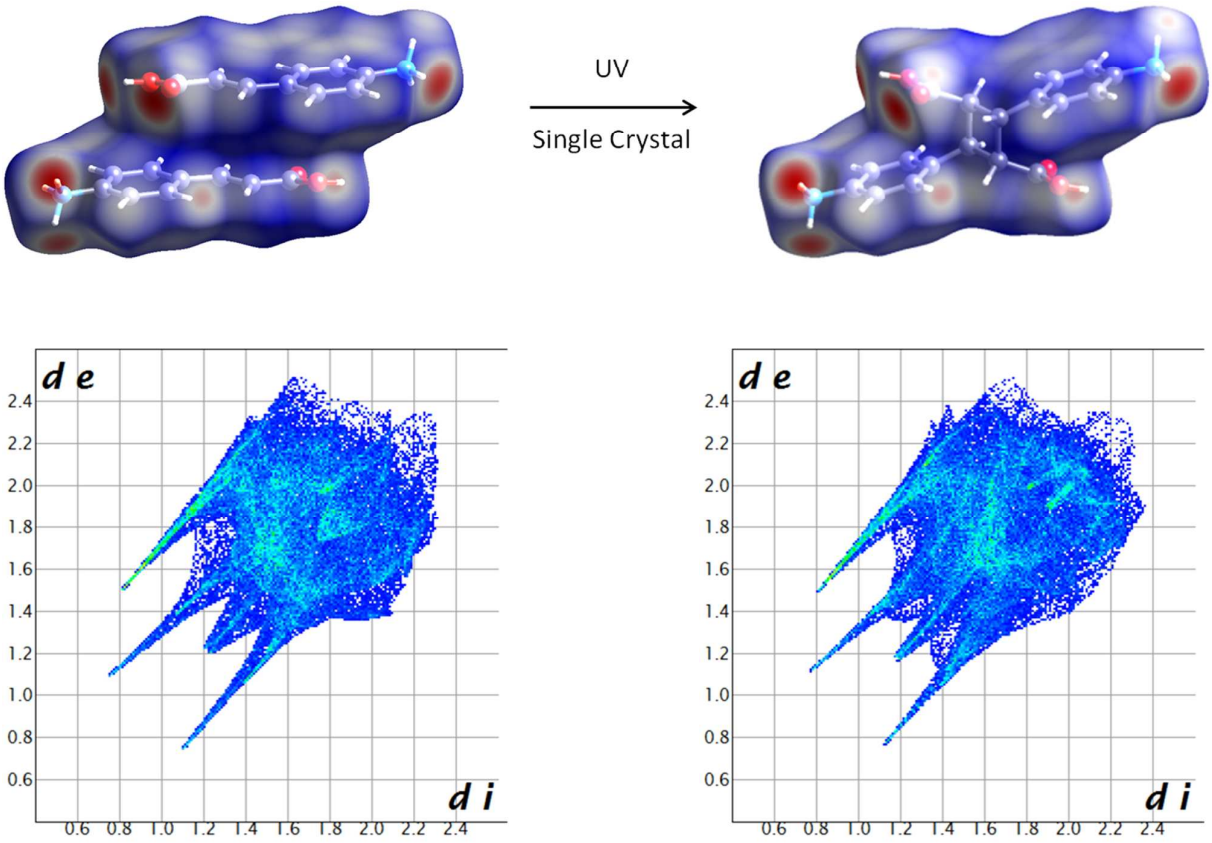

Figure SI-9. Hirshfeld Surfaces for the photoreaction [**1**H]Br form B → α-[$\mathbf{1}_2H_2$]Br_2 mapped with d_{norm}, and corresponding 2D FingerPrint plots.

Hydrogen bond and dimer content variations over the course of photoreaction [1H]Br form B → α-[1_2H_2]Br_2. During the course of the photoreaction the hydrogen bonding interactions between COOH, Br^- and NH_3^+ are almost constants. This means that no important interactions break and reform, Figure SI-10.

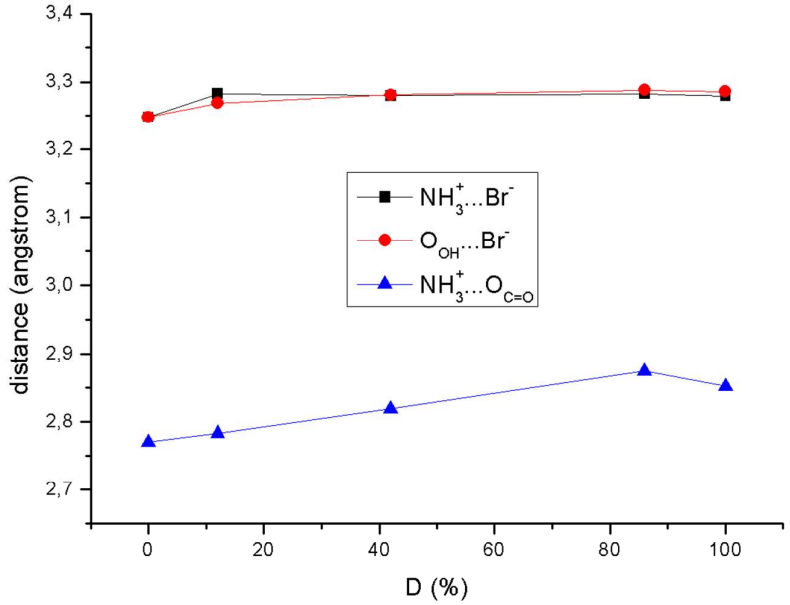

Figure SI-10.

Cell constant variations over the course of photoreaction [1H]Br form B → α-[1_2H_2]Br_2. Variation of cell parameters, together with the cell volume, upon irradiation, for each stage of photodimerization, Figure SI-11. Reaction does not require a strong rearrangement and proceeds topotactically to completion and with formation of solid solutions.

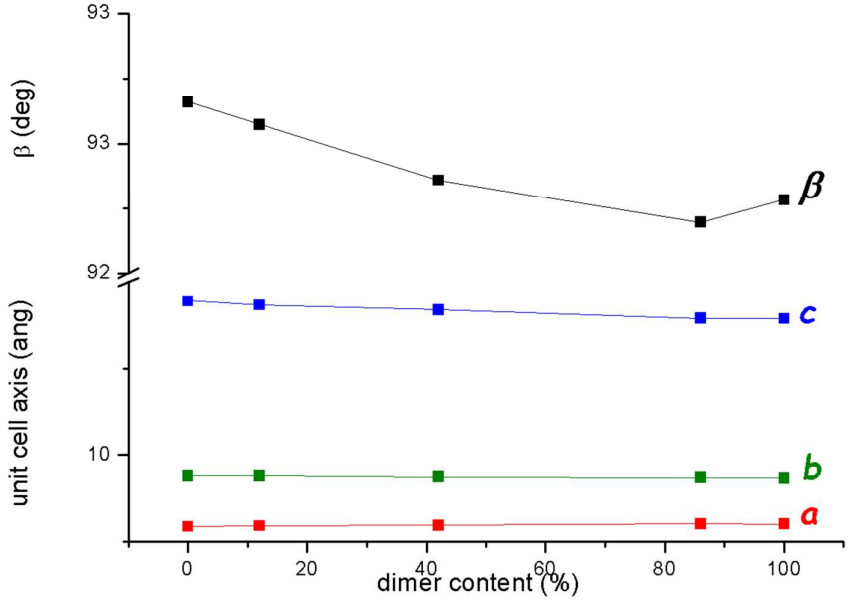

Figure SI-11. Variation of the unit cell constants and volume over the course of UV irradiation for [**1**H]Br form B.

Dimer content variations over the course of photoreaction [1H]Br form B → α-[1_2H_2]Br_2.

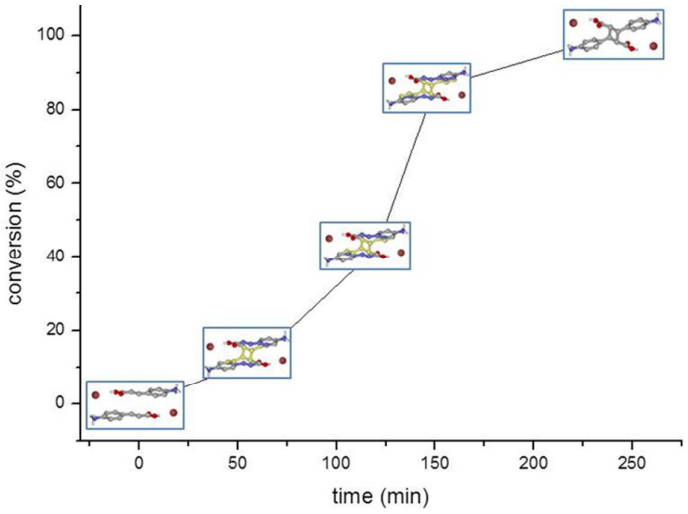

Figure SI-12.

Powder diffraction measurements. For phase identification purposes X-ray powder diffractograms in the 2θ range 5-40° (step size, 0.02°; time/step, 20 s; 0.04 rad soller; 40mA x 40kV) were collected on a Panalytical X'Pert PRO automated diffractometer equipped with an X'Celerator detector and in Bragg-Brentano geometry, using Cu Kα radiation without a monochromator. The program Mercury[2] was used for simulation of X-ray powder patterns on the basis of single crystal data. Chemical and structural identity between bulk materials and single crystals verified only for [**1**H]Br form B and α-[$\mathbf{1}_2H_2$]Br_2, by comparing experimental and simulated powder diffraction patterns (Figure SI-13).

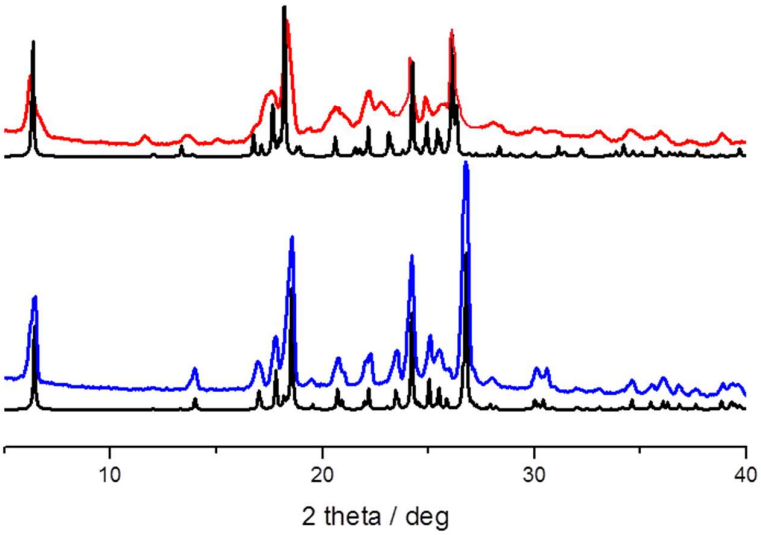

Figure SI-13. Simulated (black line) X-ray powder diffraction patterns for [**1**H]Br form B and **α-**[$\mathbf{1}_2H_2$]Br_2 and experimental for [**1**H]Br form B (blue line) and **α-**[1_2H_2]Br_2 (red line).

FTIR spectroscopy. FTIR spectra were collected using a Bruker Alpha FTIR spectrometer. FTIR spectra in the range 2000-900 cm^{-1} were run on KBr pellets (sample amount: 1-2 mg, KBr amount: 200 mg), resolution was set to 2 cm^{-1}, and 128 scans for both background and measurement were collected. Spectra were run twice, before and after overnight UV irradiation (365 nm) on the same pellet sample (Figure SI-14). These changes are in agreement with what observed by Chu and co-workers for similar systems.[8,9]

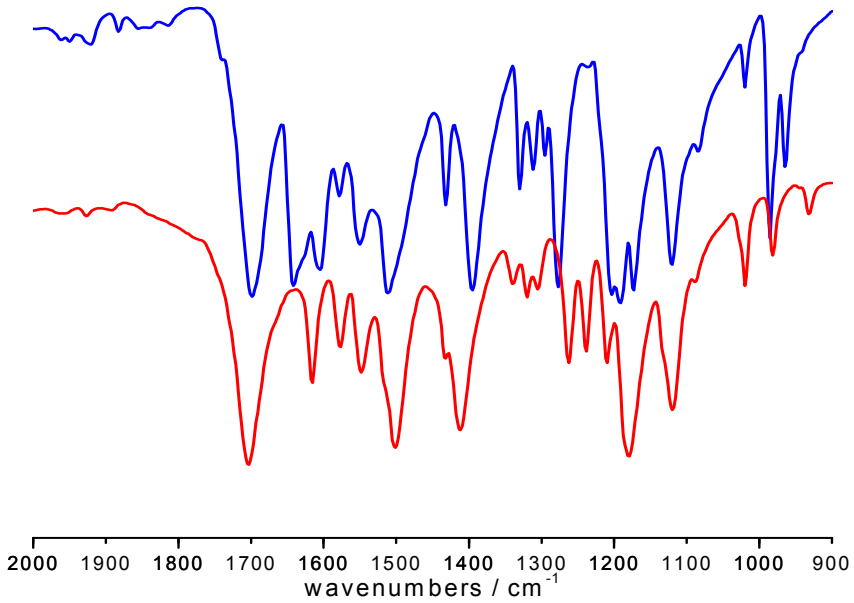

Figure SI-14. FTIR spectra of salt [**1**H]Br form B recorded before (blue line) and after (red line) overnight irradiation (365 nm) corresponding to **α-**$[1_2H_2]Br_2$.

FT-Raman spectroscopy. Raman spectra were recorded on a Bruker MultiRam FT-Raman spectrometer equipped with a cooled Ge-diode detector. The excitation source was an Nd^{3+}-YAG laser (1064 nm) in the backscattering (180°) configuration. The focused laser beam diameter was about 100 μm and the spectral resolution 4 cm^{-1}. Laser power at the sample was about 40 mW.
The spectra reported in Figure SI-15 were recorded on [**1**H]Br form B before and after overnight UV irradiation (365 nm). The changes are consistent with the occurrence of the [2+2] photodimerization, in agreement with other studies on similar systems.[10-14]

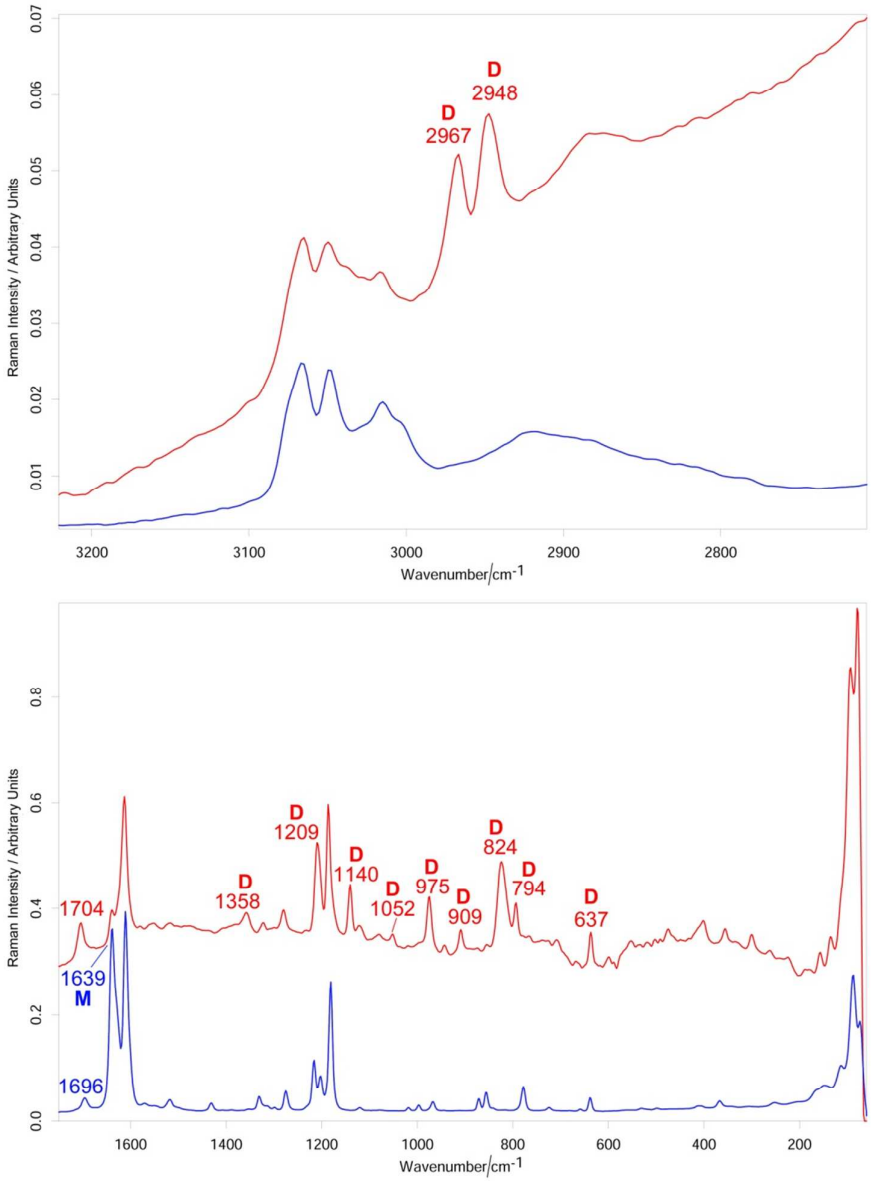

Figure SI-15. Raman spectra of salt [**1**H]Br form B recorded before (blue line) and after (red line) overnight irradiation (365 nm) corresponding to **α-**[1_2H_2]Br_2. The main bands assignable to the monomer (M) and dimer (D) are indicated; in the spectrum of the irradiated sample, the former weakened, while the latter appeared or increased in intensity. The shift of the C=O stretching mode from 1696 to 1704 cm^{-1} confirms the conversion of the C=C double bond into a C-C single bond (resulting in loss of conjugation).

NMR spectroscopy. ^{1}H NMR spectra were recorded on a Varian INOVA 400 (400 MHz) spectrometer and using, as solvent, dimethylsulfoxyde-d_6 (DMSO-d_6) bought from Sigma-Aldrich. Chemical shifts are reported in ppm using the residual solvent peak as reference. Data are reported as follows: chemical shift, multiplicity (d = doublet, m = multiplet), coupling constants (Hz), and number of protons (nH). Spectra were run on polycrystalline samples of [**1**H]Br form A, [**1**H]Br form C, obtained after prolonged (3 days) irradiation at 365 nm (Figure SI-16). Spectra were run on polycrystalline samples of [**1**H]Br form B before and after irradiation at 365 nm, (Figure SI-17).
Before irradiation - [**1**H]Br form A (DMSO-d_6, 400 Hz):7.69 (d, *J* = 8.2 Hz, 2H), 7.55 (d, J = 16 Hz,2H), 7.19 (d, *J* = 8.5 Hz, 1H), 6.45 (d, J = 16 Hz, 1H).
After irradiation - [**1**H]Br form C (DMSO-d_6, 400 Hz):7.69 (d, *J* = 8.2 Hz, 2H), 7.55 (d, J = 16 Hz,2H), 7.19 (d, *J* = 8.5 Hz, 1H), 6.45 (d, J = 16 Hz, 1H).
Before irradiation - [**1**H]Br form B (DMSO-d_6, 400 Hz):7.69 (d, *J* = 8.2 Hz, 2H), 7.55 (d, J = 16 Hz,2H), 7.19 (d, *J* = 8.5 Hz, 1H), 6.45 (d, J = 16 Hz, 1H).
After irradiation - α-[$\mathbf{1}_2H_2$]Br_2 (DMSO-d_6, 400 Hz): 7.45 (d, *J* = 7.2 Hz, 4H), 7.27 (d, J = 7.2, 4H), 4.3 (m, 2H), 3.82 (m, 2H).

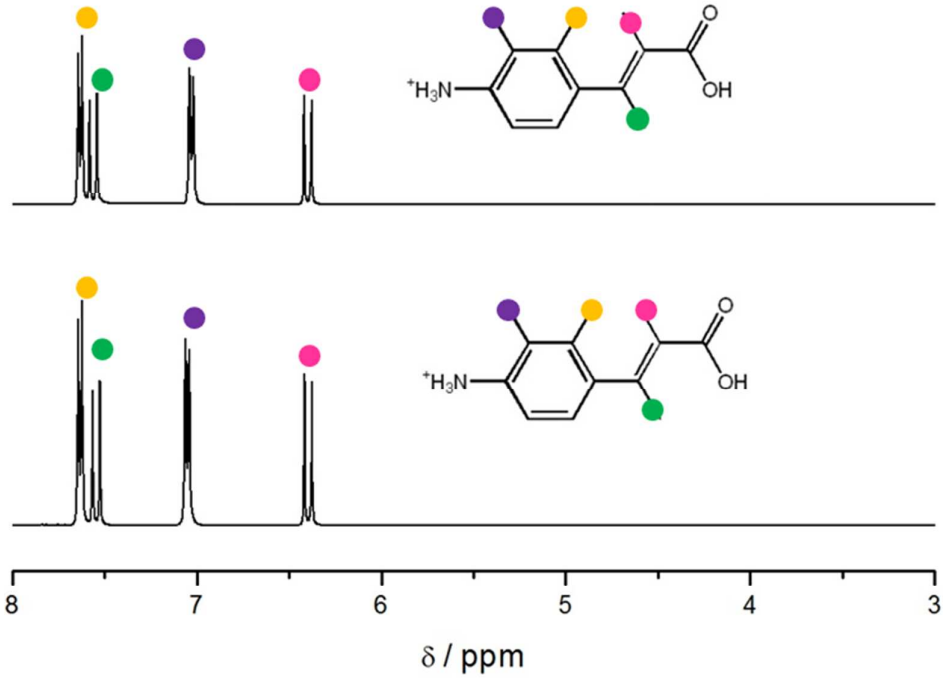

Figure SI-16. ^{1}H NMR spectra in DMSD-d_6 of [**1**H]Br form A run before (top) and after (bottom) prolonged irradiation at 365 nm, no changes are detected in [**1**H]Br form C, indicating thus that chemical identity is maintained.

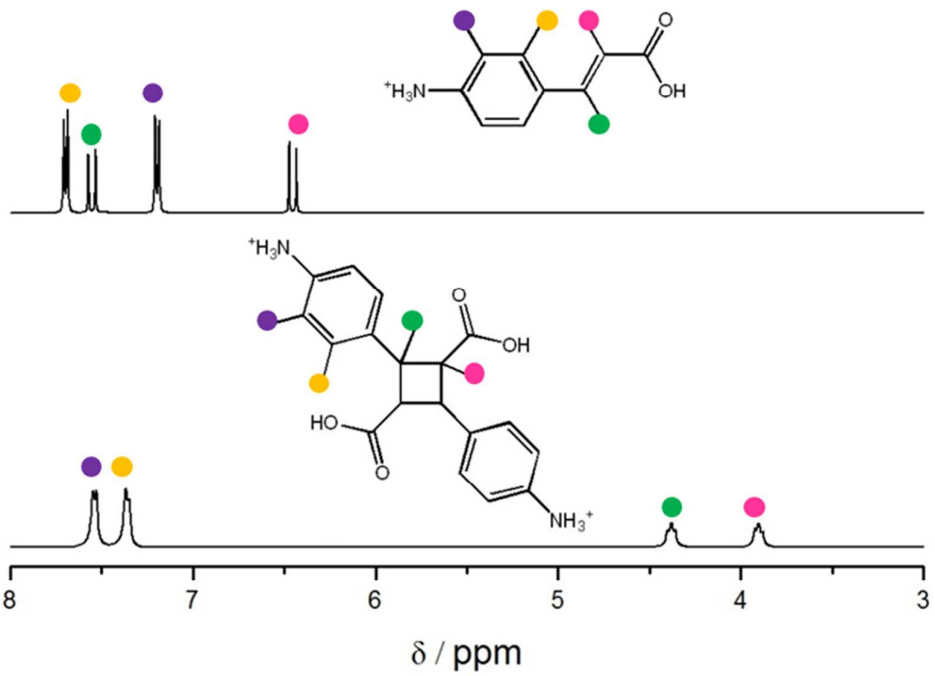

Figure SI-17. ^{1}H NMR spectra in DMSD-d_6 of [**1**H]Br form B run before (top) and after (bottom) overnight irradiation at 365 nm, the latter fully correspond to the photoproduct α-[$\mathbf{1}_2H_2$]Br_2, no traces of the starting material are detected.

References

[1] Sheldrick, G. M. SHELX97, *Program for Crystal Structure Determination*; University of Göttingen: Göttingen, Germany, 1997.

[2] Macrae, C. F.; Bruno, I. J.; Chisholm, J. A.; Edgington, P. R.; McCabe, P.; Pidcock, E.; Rodriguez-Monge, L.; Taylor, R.; van de Streek J.; Wood, P. A. Mercury CSD 2.0 – new features for the visualization and investigation of crystal structures**.** *J. Appl. Crystallogr.* 2008, *41*, 466.

[3]Cohen, M. D.; Schmidt, G. M. J.; Sonntag F. I. Topochemistry. Part II. The photochemistry of trans-cinnamic acids. *J. Chem. Soc.* **1964**, 2000.

[4] Yang, S.-Y.; Naumov, P.; Fukuzumi, S. Topochemical Limits for Solid-State Photoreactivity by Fine Tuning of the π–π Interactions. *J. Am. Chem. Soc.* **2009**, *131*, 7247.

[5] Cohelo, A., TOPAS-Academic, Coelho Software, Brisbane, Australia, 2007.

[6]Spackman, M. A.; Jayatilaka, D. Hirshfeld surface analysis. *CrystEngComm* **2009**, *11*, 19.

[7] Spackman, M. A..; McKinnon, J. J. Towards quantitative analysis of intermolecular interactions with Hirshfeld surfaces. *CrystEngComm* **2002**, *4*, 378.

[8] Wang, Z.; Randazzo, K.; Hou, X.; Simpson, J.; Struppe, J.; Ugrinov, A.; Kastern, B.; Wysocki, E.; Chu, Q. R. Stereoregular two-dimensional polymers constructed by topochemical polymerization. *Macromolecules* **2015**, *48*, 2894.

[9] Wang, Z.; Kastern, B.; Randazzo, K.; Ugrinov, A.; Butz, J.; Seals, D. W.; Sibi M. P.; Chu, Q. R. Linear polyester synthesized from furfural-based monomer by photoreaction in sunlight. *Green Chem.* **2015**, 17, 4720.
[10] Ghosh, M.; Chakrabarti, S.; Misra T. N. J. Crystalline state photoreaction in 4-methylcinnamic acid: a Raman phonon spectroscopic study. *Raman Spectrosc.* **1998,** *29*, 263.
[11] Ghosh, M.; Mandal, T. K.; Chakrabarti, S.; Misra T. N. Spectroscopic study of solid□state photoreaction in organic crystals: photopolymerization of the dimethyl ester of p□phenylenediacrylic acid. *J. Raman Spectrosc*. **1998**, *29*, 807.
[12] Allen, S. D.M.; Almond M. J.; Bruneel, J. L.; Gilbert, A.; Hollins, P.; Mascetti, J. The photodimerisation of trans-cinnamic acid and its derivatives: a study by vibrational microspectroscopy. *Spectrochim. Acta Part A,* **2000**, *56*, 2423.
[13] Atkinson, S. D.M.; Almond, M. J.; Hollins, P.; Jenkins, S. L. The photodimerisation of the α- and β-forms of *trans*-cinnamic acid: a study of single crystals by vibrational microspectroscopy. *Spectrochim. Acta Part A,* **2003**, *59*, 629.
[14] Atkinson, S. D. M.; Almond, M. J.; Bowmaker, G. A.; Drew, M. G. B.; Feltham, E. J.; Hollins, P.; Jenkins S. L.; Wiltshire K. S. The photodimerisation of the Chloro-, Methoxy- and Nitro-Derivatives of trans-Cinnamic acid: A Study of Single Crystals by vibrational Microspectroscopy. *J. Chem. Soc*., *Perkin Trans.* **2002**, *2*, 1533–1537.